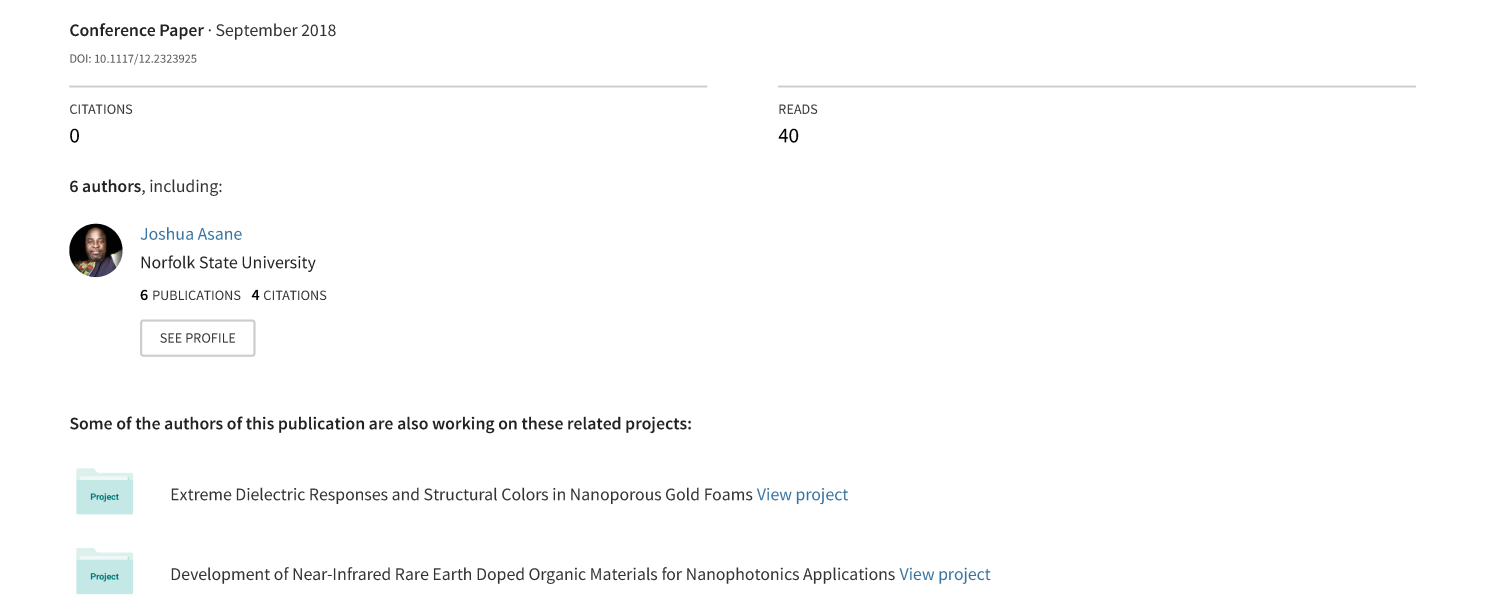
Study of conductivity of the poly(3-hexylthiophene-2, 5-diyl) polymer (P3HT) in resonant Fabry-Perot cavities



PROCEEDINGS OF SPIE

SPIEDigitalLibrary.org/conference-proceedings-of-spie

Study of conductivity of the poly(3-hexylthiophene-2, 5-diyl) polymer (P3HT) in resonant Fabry-Perot cavities

J. K. Asane, V. N. Peters, R. Alexander, T. Wallace, D. A. Peters, et al.

J. K. Asane, V. N. Peters, R. Alexander, T. Wallace, D. A. Peters, M. A. Noginov, "Study of conductivity of the poly(3-hexylthiophene-2, 5-diyl) polymer (P3HT) in resonant Fabry-Perot cavities," Proc. SPIE 10719, Metamaterials, Metadevices, and Metasystems 2018, 1071934 (24 September 2018); doi: 10.1117/12.2323925



Event: SPIE Nanoscience + Engineering, 2018, San Diego, California, United States

Study of electrical conductivity of the poly(3 hexylthiophene-2, 5-diyl) polymer (P3HT) in resonant Fabry-Perot cavities

J. K. Asane¹, V. N. Peters¹, R. Alexander^{2,3}, T. Wallace^{1,2}, D. A. Peters^{2,4}, M. A. Noginov^{1*}

Abstract

Enhancing electrical conductance in organic semiconductors has been a focus of intense research over last few decades. The improvement can be made by optimizing either the material or the device architecture. As it has been shown in [Orgiu et al., Nature Materials, 2015], strong coupling of organic molecules with a nanostructured plasmonic substrate can significantly improve the molecules' electrical conductivity. In the present study, we searched for the effect of strong coupling with a Fabry-Perot cavity on the conductivity of the semiconducting Poly (3-hexylthiophene) (P3HT) polymer. Despite the observation of the strong coupling evidenced by a very large Rabi splitting of 1.0 eV, the increase of electrical conductivity with increase of the P3HT film thickness was primarily affected by an increase of the polymer's order in thick P3HT films.

Keywords

Strong coupling, Poly (3-hexylthiophene-2, 5-diyl) polymer, conductivity, resonant cavity

1. Introduction

Recently, organic semiconducting polymers have been at the center of intense industrial and academic research, due to their ability to create flexible and inexpensive devices that can be processed on a large scale. Such devices are to be used in thin-film transistors, photoelectrical cells, light emitting diodes, photovoltaics, plasmonic devices, photoelectrical cells and many more electronic applications. However, the widespread adoption of these materials into electronic systems is hindered by the very low charge carrier mobility, which is associated with large disorder in organic materials, as compared to conversional inorganic semiconductors. Light-matter interaction enters the strong coupling regime when the photon exchange rate between exciton and electromagnetic modes becomes faster than the decay and/or decoherence rates of either constituent. Strong coupling leads to the formation of two hybridized light-matter

Metamaterials, Metadevices, and Metasystems 2018, edited by Nader Engheta, Mikhail A. Noginov, Nikolay I. Zheludev, Proc. of SPIE Vol. 10719, 1071934 © 2018 SPIE · CCC code: 0277-786X/18/\$18 · doi: 10.1117/12.2323925

polaritonic states, P₊ and P₋ separated by the energy gap known as the Rabi splitting, Fig.1. In

¹Center for Materials Research, Norfolk State University, Norfolk, VA 23504

²Summer research program, Center for Materials Research, NSU, Norfolk, VA 23504

³School of Engineering, University of Michigan, Ann Arbor, MI 48109

⁴College of Science, Purdue University, West Lafayette, IN 47907

^{*}Correspondence: mnoginov@nsu.edu

quantum electrodynamics, the Rabi splitting (for a single molecule) is proportional to $\sqrt{n_{ph}+1}$, where n_{ph} is the number of photons in the mode. This means that even in the dark, there always exists a finite Rabi splitting attributed to the interaction with vacuum fluctuations.

Light-matter interaction in the strong coupling regime offers exciting possibilities for exploring a broad range of physical phenomena, including Bose-Einstein condensation in organic and inorganic semiconductors ⁹, modification of chemical reactivities ¹⁰ and surface potentials ¹¹, Fano resonances ¹², Förster energy transfer ¹³, spontaneous ¹⁴ and stimulated ¹⁵ emission, and van der Waals interactions ¹⁶. Strong coupling of *e.g.* molecular ensembles with electromagnetic modes can be achieved by utilizing surface plasmon resonances or confined electromagnetic environments, such as cavities. A typical example of a strongly coupled system is a Fabry-Perot (micro) cavity (composed of two parallel metallic mirrors), which is resonant with an electronic transition in a dye-doped polymer or an organic semiconductor filling the cavity. Large molecular concentrations and collective dipole moments lead to gigantic Rabi splitting (as large as 1.12 eV ¹⁷), which are comparable with energy eigenvalues of not coupled constituents taken separately. The latter light-matter interaction is said to occur in the ultrastrong coupling regime.

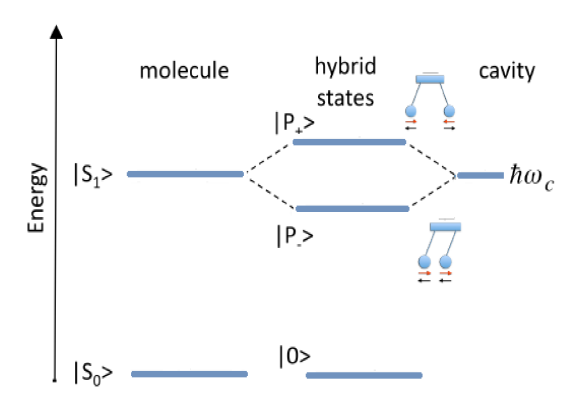


Fig. 1. The simplified energy diagram showing the interaction of a HOMO-LUMO (S_0 – S_1) transition of a molecule resonant with a cavity mode $\hbar\omega_c$, where ω_c is the resonant oscillation frequency of the cavity. Strong coupling leads to the formation of two hybrid light–matter (polaritonic) states (P- and P₊) separated by the Rabi splitting energy $\hbar\Omega_R$. 0 represents the ground state.¹⁸

According to Ref. [7], large ensembles ($\sim 10^5$) of organic molecules can be strongly coupled to plasmonic modes, resulting in an increase of electrical conductivity. We asked the question whether this phenomenon is universal and whether it should be expected in other strongly coupled systems involving organic molecules and polymers.

In the present study, we searched for the effect of strong coupling (with Fabry-Perot cavities) on electrical conductivity of Poly(3-hexylthiophene-2,5-diyl) polymer (P3HT). Despite the

remarkably strong coupling (Rabi splitting ~1.0 eV), no correlation between the strong coupling and the electrical conductivity has been found. The only effect on the electrical conductivity was (tentatively) from increase of the order in thick P3HT films.

2. Experimental Samples and Measurements

2.1 Sample fabrication

We designed and experimentally fabricated multiple resonant Fabry-Perot cavities by sandwiching 2,5-poly(3-hexylthiophene) (P3HT) semiconducting polymeric films of different thickness between thick bottom silver layer (deposited onto a glass substrate) and a thin semi-transparent top silver layer, Fig. 2. The metallic Ag films were deposited on clean glass substrates using thermal evaporator (Edwards coating, Auto306) and all film thicknesses were measured with the Bruker DektakXT profilometer. The polymeric solutions were prepared from a high purity, 99.995%, P3HT flakes (with molecular weight ~40kD and head-to-tail regioregularity >99%, obtained from Sigma Aldrich) dissolved in ACS grade chloroform from Fisher Scientific.

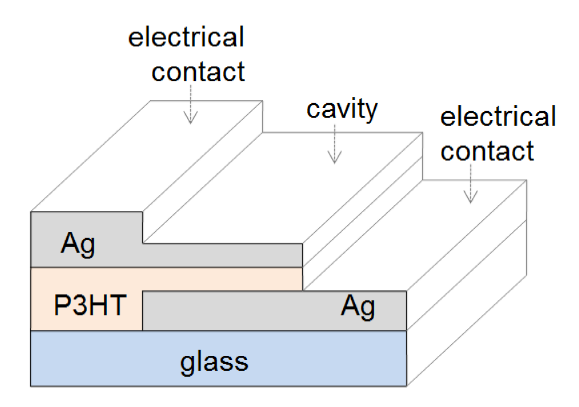


Fig. 2. Schematics of the Fabry-Perot cavity: bottom layer Ag ~ 200 nm and the top semi-transparent Ag layer ~ 40 nm sandwiching polymeric P3HT films of different thicknesses.

2.2 Numerical modeling of resonant cavities

Numerical solutions to Maxwell equations were obtained using the commercial finite element method (FEM) solver, COMSOL Multiphysics. The spectra of real and imaginary parts of the dielectric permittivity of Ag were obtained from Ref. [19], and those of the P3HT polymer were adopted from Ref. [20] The reflectance spectra of Fabry-Perot cavities of difference sizes filled with P3HT were calculated and the energy positions of the dips in the reflectance spectra were plotted against the cavity thickness d, forming two branches of the dispersion curve with a Rabi splitting, Fig. 3.

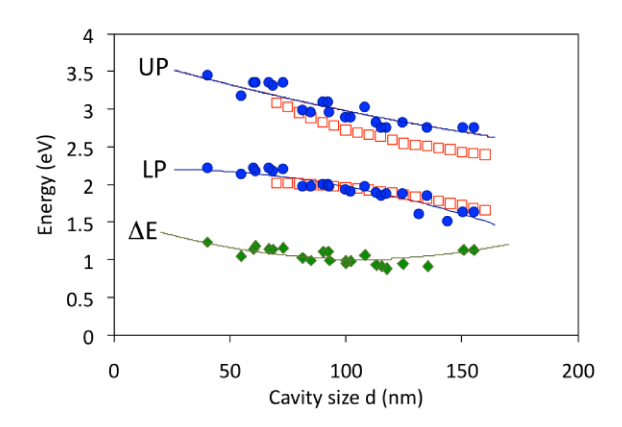


Fig. 3. Dependence of the spectral positions of the reflectance dips on the cavity size d. UP is the upper polariton branch, LP is the lower polariton branch, and ΔE =UP-LP is the difference between them. Red open squares – calculation, blue closed circles and green filled diamonds – experiment, solid lines – guides for eyes.

2.3 Optical studies

The reflectance spectra of the experimental samples were measured in the integrated sphere of the Lambda 900 spectrophotometer. Two minima in the reflectance spectra, manifesting the strong coupling, have been observed in most of the samples studied. The corresponding experimental dispersion curve, characterized by one of the largest Rabi splittings reported in the literature, 1.0 eV, was in a good agreement with that calculated numerically, Fig. 3.

The absorbance spectra taken in the series of P3HT films of different thickness (deposited on glass) reveal known in the literature structure of the P3HT absorption band, featuring maxima and shoulders at 520 nm, 550 nm and 600 nm in thicker films, while the absorbance spectra of thinner P3HT films were nearly featureless, Fig. 4. This suggests that thick films have higher degree of crystallinity than thin films ²¹.

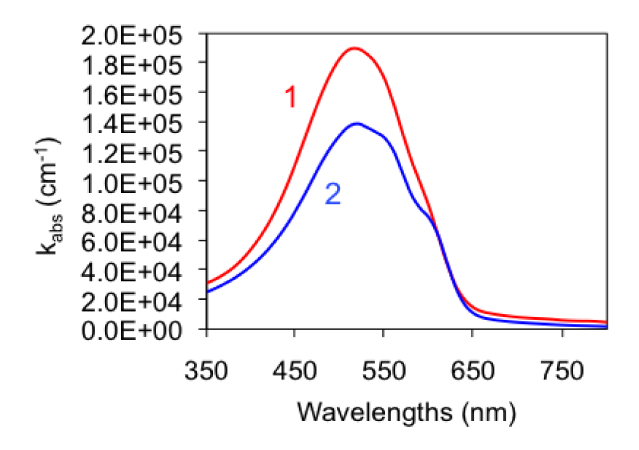


Fig. 4. Absorption spectra indicating increase of crystallinity with increase of the thickness of P3HT films deposited onto glass substrates; trace1: film thickness ~ 76 nm; trace 2: film thickness ~ 255 nm.

2.4 Electrical studies

The current-voltage (I-V) response of the cavity samples, measured in a straightforward setup involving dc voltage supply from Xantrex, voltmeter and ammeter (both 34405A Multimeters from Agilent), was found to be linear or ohmic in nature, Fig. 5.

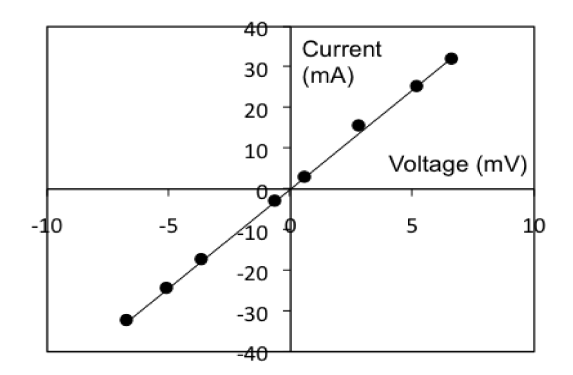


Fig. 5. Typical I-V curve of the Fabry-Perot cavity filled with the P3HT polymer.

Alternatively, the dc resistance of P3HT cavity samples, R, was routinely measured using the digital multimeter (model 34405A from Agilent) switched to the ohmmeter mode. The resistance of Ag films and other electrical conduits, measured in the schematics of Fig. 2 without P3HT layer, was properly taken into account. The electrical conductivity of the samples studied was calculated from the Pouillet's relation, $\sigma_{dc} = \frac{L}{RA_c}$, where σ_{dc} is the dc conductivity, A_c is the

cross-sectional area of the P3HT cavity and L is the thickness of the P3HT layer.

In our experiments, we used two nominally identical batches of P3HT (from Sigma Aldrich). The results of their electrical conductivity studies are summarized in Figs. 6a and 6b. We have found that: (i) In both series of samples, the measured values of electrical conductivity fell within the range of data reported in the literature between 10⁻⁴ S/cm and 10⁻⁹ S/cm. (ii) There is no any obvious correlation between the size dependence of the electrical conductivity and the behavior of the dispersion curve. In particular, no anomaly in the electrical conductivity is observed at the cavity size equal to ~100 nm, when the energy gap between the upper and the lower polariton branches is the smallest (Fig. 3, green diamonds) and the coupling is the strongest. (iii) The only observable trend was the increase of electrical conductivity with the increase of the cavity size, Fig. 6. As electrical conductivity is expected to increase with an increase in the polymer's crystallinity ³⁰, the latter phenomenon can tentatively explain our experimental results.

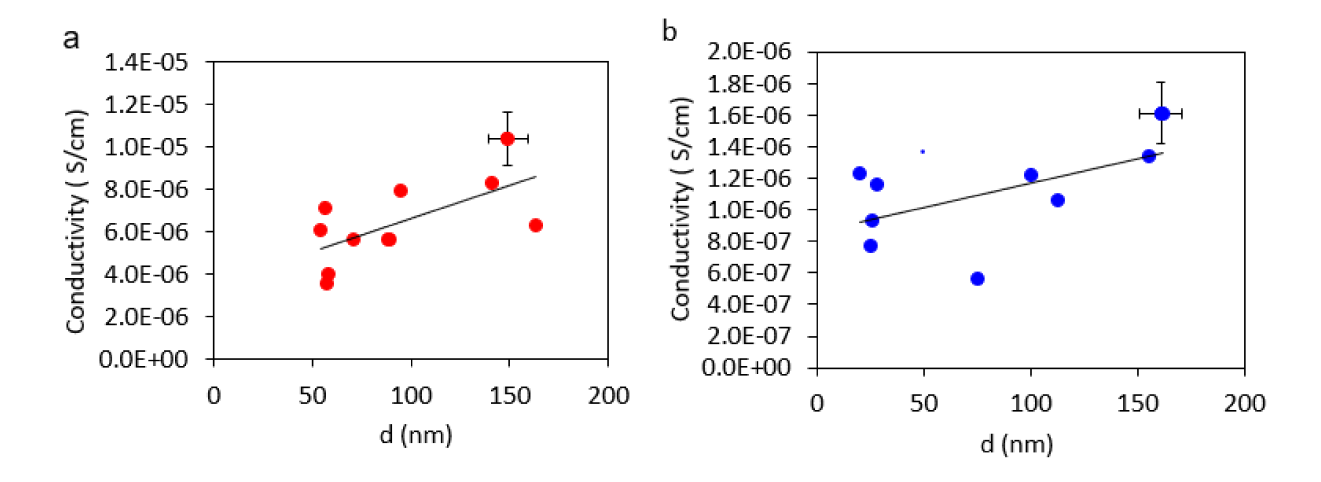


Fig. 6. Electrical conductivity as a function of the thickness of the P3HT layers, measured in samples fabricated from two batches of the P3HT polymer.

3. Summary

We have studied electrical conductivity of P3HT polymeric films, which were stronger or weaker coupled to Fabry-Perot cavities. Despite the observation of a gigantic strong coupling evidenced by the Rabi splitting of 1.0 eV, no obvious correlation was found between the strong coupling and the electrical conductivity. The latter was (presumably) primarily affected by an increase of the polymer's crystallinity in thick P3HT films. On the other hand, since the upper and the lower polariton branches of the dispersion curve (as well as the difference between them) were nearly flat and featureless, Fig. 3, observation of any sharp anomalies in thickness-dependent electrical conductivity could not be expected. Therefore, we conclude that the effect of strong coupling on electrical conductivity of molecular ensembles, reported in Ref. [7], is not universal and not readily observed in every strongly coupled system.

Acknowledgments This work was supported by the NSF grants 1205457 and 1646789, AFOSR grant FA9550-14-1-0221, and ARO grant W911NF-14-1-0639.

References

¹J. Zhao, Z. Chi, Z. Yang, X. Chen, M. S. Arnold, Y. Zhang, J. Xu, Z. Chi and M. P. Aldreda Nanoscale, 10, 5764 (2018)

²L.-L. Chua, J. Zaumseil, J.-F. Chang, E.C.-W. Ou, P.K.-H. Ho, H. Sirringhaus, and R.H. Friend, Nature 434, 194 (2005).

³K. M. Coakley and M.D. McGehee, Chem. Mater. 16, 4533 (2004).

⁴I. McCulloch, R.S. Ashraf, L. Biniek, H. Bronstein, C. Combe, J.E. Donaghey, D.I. James, C.B. Schroeder and W. Zhang, Acc. Chem. Res, **45**, 714 (2012)

- ⁵Nielsen, B.C. Schroeder, and W. Zhang, Acc. Chem. Res. 45, 714 (2012).
- ⁶Y. R. Leroux, J. C. Lacroix, K. I. Chane-Ching, C. Fave, N. Félidj, G. Lévi, J. Aubard, J. R. Krenn, and A. Hohenau, J. Am. Chem. Soc. 127, 16022 (2005).
- ⁷E. Orgiu, J. George, J. A. Hutchison, E. Devaux, J. F. Dayen, B. Doudin, F. Stellacci, C. Genet, J. Schachenmayer, C. Genes, G. Pupillo, P. Samorì & T. W. Ebbesen; Nat. Mater. **14**, 1123 (2015)
- ⁸P. Törmä and W. Barnes; Rep. Prog. Phys. **78**, 013901(2015)
- ⁹D. W. Snoke, and J. Keeling; Physics Today 70, **10**, 54 (2017)
- ¹⁰P. Vasa and C. Lienau; ACS Photonics 5, 2(2018)
- ¹¹J. A. Hutchison, A. Liscio, T. Schwartz, A. Canaguier-Durand, C. Genet, V. Palermo, P. Samorì, and T. W. Ebbesen, Adv. Mater. **25**, 2481(2013)
- ¹²T. J. Arruda, A. S. Martinez, and F. A. Pinheiro, Phys. Rev. A, **87**, 043841 (2013)
- ¹³T. Tumkur, J. Kitur, C. E. Bonner, A. Poddubny, E. E. Narimanov, and M. A. Noginov, Faraday Disc Soc **178**, 395(2015)
- ¹⁴Z. Jacob, J.-Y. Kim, G. V. Naik, A. Boltasseva, E. E. Narimanov, V. M. Shalaev, Applied Physics 100, 215(2010).
- ¹⁵J. K. Kitur, L. Gu, T. Tumkur, C. E. Bonner and M. A. Noginov, ACS Photonics **2**, 1019(2015)
- ¹⁶S. A Maier, *Plasmonics: Fundamentals and Applications* (2007)
- ¹⁷S. Gambino, M. Mazzeo, A. Genco, O. Di Stefano, S. Savasta, S. Patanè, D. Ballarini, F. Mangione, G. Lerario, D. Sanvitto, G. Gigli, ACS Photonics, 1, 1042(2014)
- ¹⁸J.A. Hutchison, T. Schwartz, C. Genet, E. Devaux, and T.W. Ebbesen, Angew. Chemie Int. Ed. 51, 1592 (2012)
- ¹⁹P. B. Johnson and R. W. Christy, Phy. Rev.**6**, 4370(1972)
- ²⁰V. N. Peters, T. U. Tumkur, G. Zhu, M. A. Noginov, Sci. Rep. **5**, 14620 (2015)
- ²¹K. Sakamakib, K. Akagib, H. Shirakawab, H. Kyotani, Syn. Met. **84**, 365 (1997)
- ²²J. Obrzut and K. A. Page, Phys. Rev. B, **80**, 195211 (2009).
- ²³B. K. Kuila and A. K. Nandi, Macromolecules **37**, 8577 (2004).
- ²⁴A. J. Mozer, N. S. Sariciftci, A. Pivrikas, R. Österbacka, G. Juška, L. Brassat and H. Bässler, Phys Rev B, **71**, 035214 (2005)
- ²⁵F. Yakuphanoglu and B. F. Senkal; J. Polym Eng Sci: Newtown: **49**, 722 (2009)

- ²⁶J. Cui, D.E. Martínez-Tong, A. Sanz, T.A. Ezquerra, E. Rebollar, and A. Nogales, Macromolecules **49**, 2709 (2016).
- ²⁷J. Hynynen, D. Kiefer, L. Yu, R. Kroon, R. Munir, A. Amassian, M. Kemerink, and C. Müller, Macromolecules **50**, 8140 (2017).
- ²⁸W. Meng, R. Ge, Z. Li, J. Tong, T. Liu, Q. Zhao, S. Xiong, F. Jiang, L. Mao, and Y. Zhou, ACS Appl. Mater. Interfaces **7**, 14089 (2015).
- ²⁹J. Cui, D.E. Martínez-Tong, A. Sanz, T.A. Ezquerra, E. Rebollar, and A. Nogales, Macromolecules **49**, 2709 (2016).
- ³⁰V. Saini, Z. Li, S. Bourdo, E. Dervishi, Y. Xu, X. Ma, V.P. Kunets, G.J. Salamo, T. Viswanathan, A.R. Biris, D. Saini, and A.S. Biris, J. Phys. Chem. C **113**, 8023 (2009).